THE DYNAMICAL INFLUENCE OF THE TRANSITION REGION AND CHROMOSPHERE ON THE HEATING OF CORONAL LOOPS BY RESONANT ABSORPTION OF ALFVÉN WAVES

A.J.C. Beliën[1], **P.C.H. Martens**[2], **R. Keppens**[1]

[1]FOM-Institute for Plasma Physics 'Rijnhuizen', P.O. Box 1207, 3430 BE Nieuwegein, The Netherlands
[2]Department of Physics, Montana State University, Bozeman, MT, USA

ABSTRACT

We present and discuss some results of a numerical 2.5D MHD study of coronal loop heating by resonant absorption of Alfvén waves using a model that includes an extended chromosphere and dynamical transition region. Using the ratio of the Ohmic dissipation in the corona over the injected Poynting flux (both time integrated) as a measure of the efficiency of the resonant absorption process, it is found that this ratio is only a few percent. As such, resonant absorption does not appear to be able to explain coronal heating since it would require huge Poynting fluxes, in excess of 10^4 Wm^{-2}, at the chromospheric base of our model to balance the radiative losses in the quiet corona. Those fluxes have not been observed. It is shown that the low efficiency is mainly due to very effective energy transfer from the Alfvén waves to nonlinearly generated slow magnetoacoustic waves, especially in the chromosphere and transition region.

Key words: MHD — waves — Sun: corona — Sun: transition region — Sun: chromosphere

1. INTRODUCTION

In the last fifteen to twenty years a lot of studies have been conducted on the possibility and viability of resonant absorption of Alfvén waves as a heating mechanism for solar coronal loops (e.g., Martens 1986; Davila 1987; Hollweg & Yang 1988; Grossmann & Smith 1988; Browning 1991; Zirker 1993; Poedts & Kerner 1992; Steinolfson & Davila 1993; Ruderman & Goossens 1993; Poedts et al. 1994; Ofman et al. 1994; Halberstadt & Goedbloed 1995a; Halberstadt & Goedbloed 1995b; Ofman et al. 1995a; Ofman & Davila 1995b; Poedts & Boynton 1996; Poedts & Goedbloed 1997). The general outcome of these results is that resonant absorption is indeed a viable coronal heating mechanism provided that enough energy is available to drive the Alfvén waves of interest (this difficulty of resonant absorption was posed by Parker (1992), see Goedbloed (1995) for a counter argument) and that the magnetic Reynolds number is at least a few orders of magnitude lower than the usually assumed value in the range of 10^{10}–10^{12}. See, however, Ofman et al. (1999) for some interesting new observationally obtained values of the magnetic Reynolds number that are of the order of 10^6. The statement on the viability of resonant absorption relies, however, on the exploited coronal loop models. Studies have either been performed in slab geometry or in cylindrical geometry with, initially, only a variation of the Alfvén speed *across* the magnetic field and without any modeling of the coupling to the transition region and chromosphere. Mostly, the effects of the dense chromosphere and photosphere on the coronal wave dynamics are modeled via line-tying boundary conditions. Hence, this approach assumes that coronal cavity leakage (Hollweg 1984; Berghmans & De Bruyne 1995) and resonance detuning by length changes of the coronal cavity due to transition region motions are negligible on the time scales of interest, i.e., the time it takes for the gradients in the resonant layer to become large enough that dissipation starts to become important. This can only be satisfied for long coronal loop structures $\sim$ 100 Mm and small magnetic Reynolds numbers $\sim 10^5$, (e.g., Berghmans & De Bruyne 1995). Another reason to expect lower efficiencies is the fact that the Alfvén wave dynamics will be most nonlinear in the transition region and chromosphere since the Alfvén speed is lower in those areas and the plasma beta much higher. This allows for considerable energy transfer from Alfvén waves to magnetoacoustic waves resulting in a Poynting flux at the coronal base that is only a fraction of the one injected at the chromospheric level. It turns out that the latter is indeed very important and that it plays a major role in determining the efficiency of the heating process.

2. LOOP MODEL

We describe our model of a coronal loop briefly. For more details see Beliën et al. (1999).

Our coronal loop model is a straight cylindrical flux tube of length L with the end planes representing the chromospheric regions to which both legs of the loop are connected. The corona is located in between. The usual, projected form of gravity is exploited so that the gravitational force points towards the chromospheric end planes in both legs.

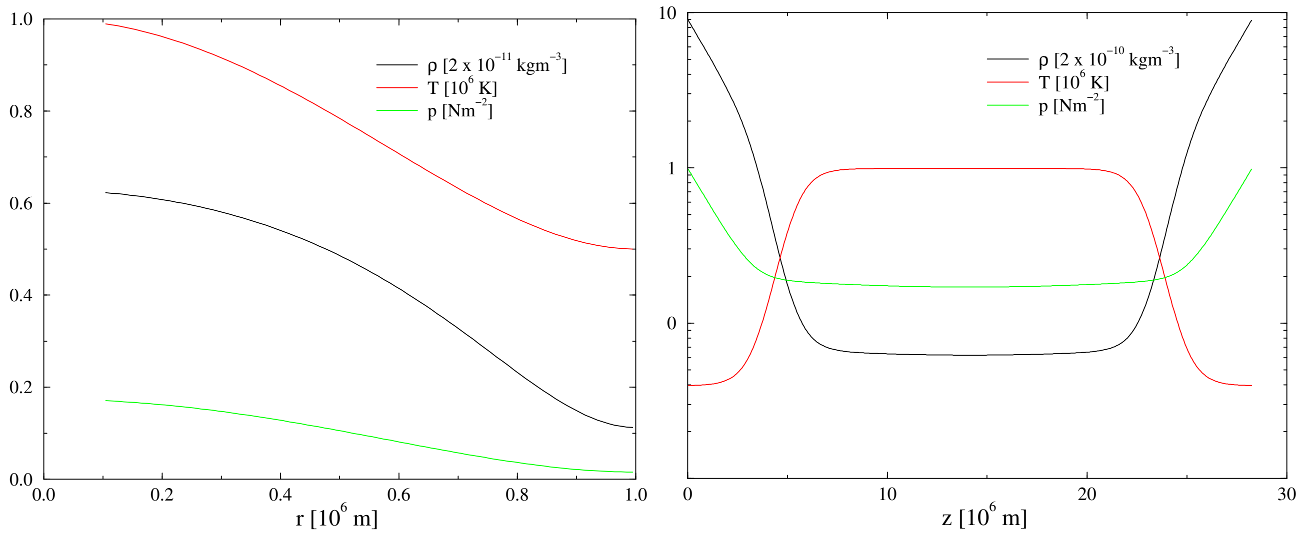

Figure 1. Radial (left) and longitudinal (right) variation of the density, ρ, the temperature, T, and the pressure, p, of the initial state. The magnetic field is nearly constant, untwisted, and mainly directed in the longitudinal direction (deviations only occur in the chromosphere where there is a small non-zero radial magnetic field due to the influence of gravity). The strength of the coronal magnetic field on axis is $B_0 = 25 \times 10^{-4}$ T.

As an initial state a numerical solution of the generalized Grad-Shafranov equation for an untwisted magnetic field is used. The resulting magnetic field is nearly constant and directed along the loop axis. The radial and longitudinal dependence of the density, temperature, and pressure are shown in Fig. 1. The radial variation of the density sets up the necessary variation of the Alfvén speed across the magnetic field so that resonant absorption can occur.

At times $t > 0$ linearly polarized mono-periodic Alfvén waves are launched at the chromospheric end plane $z = 0$ by prescribing the azimuthal velocity v_θ. The excitation is confined to the region $0.3 < r/a < 0.9$. The period of the Alfvén waves is 66.7 s. It is chosen such that the resonant layer is located somewhere in the region $0.6 < r/a < 0.7$. The amplitude of the excitation profile is 11.8 km/s.

3. NUMERICAL RESULTS

The numerical results discussed in the next subsections were obtained with the Versatile Advection Code (Tóth 1996) using a Total Variation Diminishing method based on Roe's approximate Riemann solver (Roe 1981). A resolution of 100×400 has been used. The high resolution in the longitudinal direction is necessary to be able to resolve both the sharp transition region and the occurring slow shocks well. The value of the exploited constant resistivity is determined by the dimensionless Lundquist number $S = \mu_0 v_A a/\eta$ which is approximately 8×10^4 in our simulations.

3.1. SPATIAL EVOLUTION

The spatial evolution of $\log T$, $\log \rho$, v_z, and v_θ is shown in Fig. 2.

From the spatial evolution it is evident that the amplitude of v_θ in the resonant layer around $r/a \approx 0.65$ does not grow in time. It has already reached its maximum at 283 s corresponding to approximately 4 driving periods. This is too short to be explained by cavity leakage since for the given Alfvén speed stratification in our model, an equivalent three layer model would predict 10 driving periods as a typical time scale on which the amplitude in the resonant layer would have come to within 10% of its limiting value (Berghmans & De Bruyne 1995). Also, cavity detuning cannot explain the short time scale since significant detuning only starts to play a role after the amplitude in the resonant layer has already levelled off. This is clear from the temperature and density plots that show that the uplifting of the transition region and the "spicule" formation has only started just before $t = 283$ s. The explanation of the fast levelling off lies in energy transfer from the Alfvén waves to magnetosonic waves, in particular the slow ones. In the corona these slow waves steepen into shocks as can be seen from the plots of v_z in Fig. 2. A large part of the energy of the slow waves that are generated in the chromosphere and transition region is used to transport mass from the chromosphere into the corona and, hence, to increase the internal and gravitational energy of the corona. The increased coronal pressure will help balance the large Alfvén wave pressure in the chromosphere and transition region.

3.2. ENERGY BALANCE

Studying the evolution of the quantities appearing in the energy balance equation

$$S + F = E + G$$

gives additional insight into the process that is behind the fast saturation of the Alfvén wave amplitude in the resonant layer. Here,

$$S \equiv \int^t \int_A \mathbf{E} \times \frac{\mathbf{B}}{\mu_0} \cdot d\mathbf{A} dt'$$

is the time integrated Poynting flux,

$$F \equiv \int \int_A \left(\rho \mathbf{v}^2/2 + \rho\Phi + \gamma p/(\gamma - 1)\right) \mathbf{v} \cdot d\mathbf{A} dt$$

is the flow of energy flux, and E and G are the increase of the total energy (kinetic + magnetic + internal) and gravitational energy in the volume enclosed by A.

In Fig. 3 both the evolution of the volume averaged energy balance quantities, as well as the volume averaged Ohmic dissipation OD and increase of the kinetic, K, and magnetic, M, energy are plotted. Four different volumes are considered over which the averages are taken, viz., the whole loop structure, the corona plus the top half of the transition region, and two coronal volumes.

From Fig. 3 it becomes clear that the increase of the kinetic and magnetic energy levels off after approximately four driving periods. Inspection of the graphs for the Poynting flux reveals that the slope of the total Poynting flux S for the coronal volumes becomes much smaller around the same time. This means that the instantaneous Poynting flux has dropped to a fraction of the one that is injected at the chromospheric base. Since the Alfvén waves are driven by the Poynting flux, this explains why the build up of the amplitude in the resonant layer stops. The Poynting flux injected at the chromospheric base (S for the whole volume) is almost completely converted to internal energy (as evidenced by the increase of the total energy and the levelling of the kinetic and magnetic energy) as described in the previous subsection.

The oscillations at time scales of ≈ 600 s and 150 s in the plots for the whole loop structure and the two coronal volumes are characteristic for the slow wave motions in the chromosphere and the corona, respectively. The period of the 600 s waves is just below the cut-off period of our model chromosphere and can, therefore, be regarded as a “natural” oscillation of the chromosphere.

3.3. EFFICIENCY

In the previous subsections strong indications for an inefficient heating were identified from the levelling off of v_θ, the Alfvén wave velocity component, on time scales smaller than can be explained by cavity leakage or by balancing of the energy injection into the resonant layer by Ohmic dissipation (i.e., the heating by resonant absorption). We will put it on a more quantitative base in this subsection.

Therefore, we plot the absorption α_a and dissipation coefficient α_d as a function of time in Fig. 4. These coefficients are defined as:

$$\alpha_\mathrm{d} = \frac{S}{S^+}, \qquad \alpha_\mathrm{d} = \frac{OD}{S},$$

where S is again the total time integrated Poynting flux. The Ohmic dissipation OD is given by $OD \equiv \int_V \eta j^2 \, dV$ with V an arbitrary part of the total loop volume, η the resistivity, and $\mathbf{j}$ the current density. The total time integrated *positive* Poynting flux is denoted by S^+. It can be interpreted as the total Poynting flux ‘delivered’ by the Alfvén wave driver. With these definitions, it is clear that the absorption coefficient measures the relative amount of Poynting flux that is actually absorbed by the loop. Higher values are favorable since, then, more energy is available for dissipation in the loop. The dissipation coefficient measures how much of the absorbed Poynting flux is converted into heat in a specific loop volume. Again higher values indicate better heating.

Figure 4 reveals that although a considerable part of the Poynting flux is deposited in the loop only a very small fraction, i.e., between five and ten percent, of this absorbed flux is converted into heat in the corona. Multiplying both coefficients shows that this is only a few percent of the incoming Poynting flux, i.e., very inefficient heating.

4. DISCUSSION AND CONCLUSIONS

In this paper we have presented the results of a 2.5D numerical simulation of heating by resonant absorption in a coronal loop using a loop model that includes transition and chromospheric regions at both ends of its legs. Our main goal has been to test the viability of resonant absorption for such more realistic loop models and see if its efficiency remains as high as has been found in previous investigations in which the coupling with the chromosphere was not taken into account.

Our main finding is that the efficiency of resonant absorption is very low. Only a few percent of the Poynting flux injected at the chromospheric level is actually converted into Ohmic heating. To balance the thermal losses in the quiet corona, this then would require Poynting fluxes in excess of 10^4 Wm^{-2} at the chromospheric level. However, such fluxes have not been observed (yet).

The low efficiency is mainly due to the transfer of energy from the Alfvén waves to nonlinearly generated slow magnetosonic waves. The main transfer takes place in the chromosphere and transition region where the nonlinear character of the wave dynamics is largest. Consequently, the Poynting flux carried by the Alfvén waves is only a fraction of the chromospheric one. Coronal cavity leakage and detuning play a less important role in determining the low efficiency. For the relatively small loop structure considered in this paper, cavity detuning does have an influence on the precise evolution of the magnetic

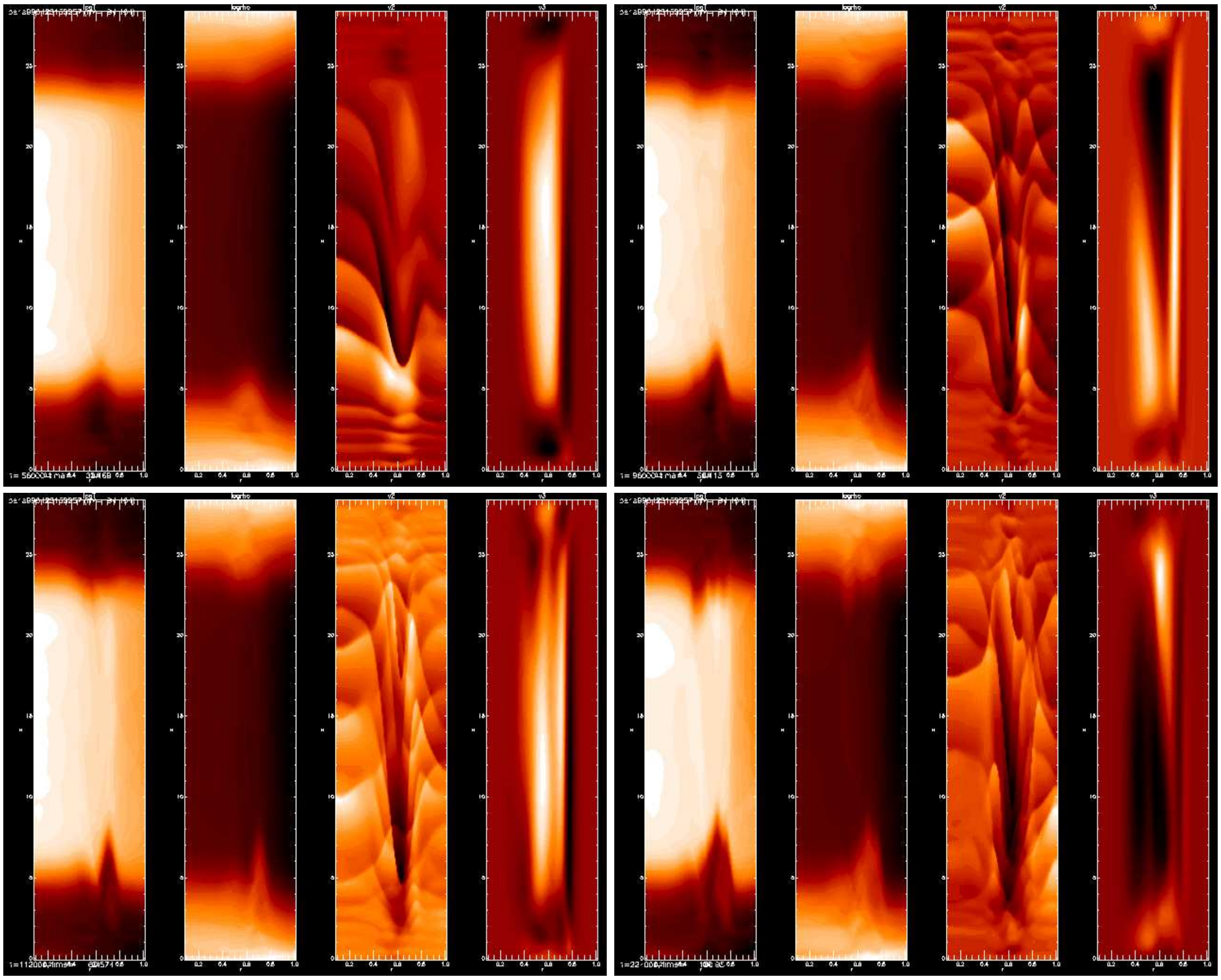

Figure 2. The spatial dependence of $\log T$, $\log \rho$, v_z, and v_θ (from left to right in each panel) plotted for four different time steps: $t = 283$ s (top left), $t = 479$ s (top right), $t = 559$ s (bottom left), and $t = 1117$ s (bottom right). Horizontally, the radial and vertically the longitudinal dependence is plotted. The minimum/maximum values of v_z and v_θ are ± 40 km/s and ± 100 km/s respectively. In all frames, white represents maximum and black minimum values.

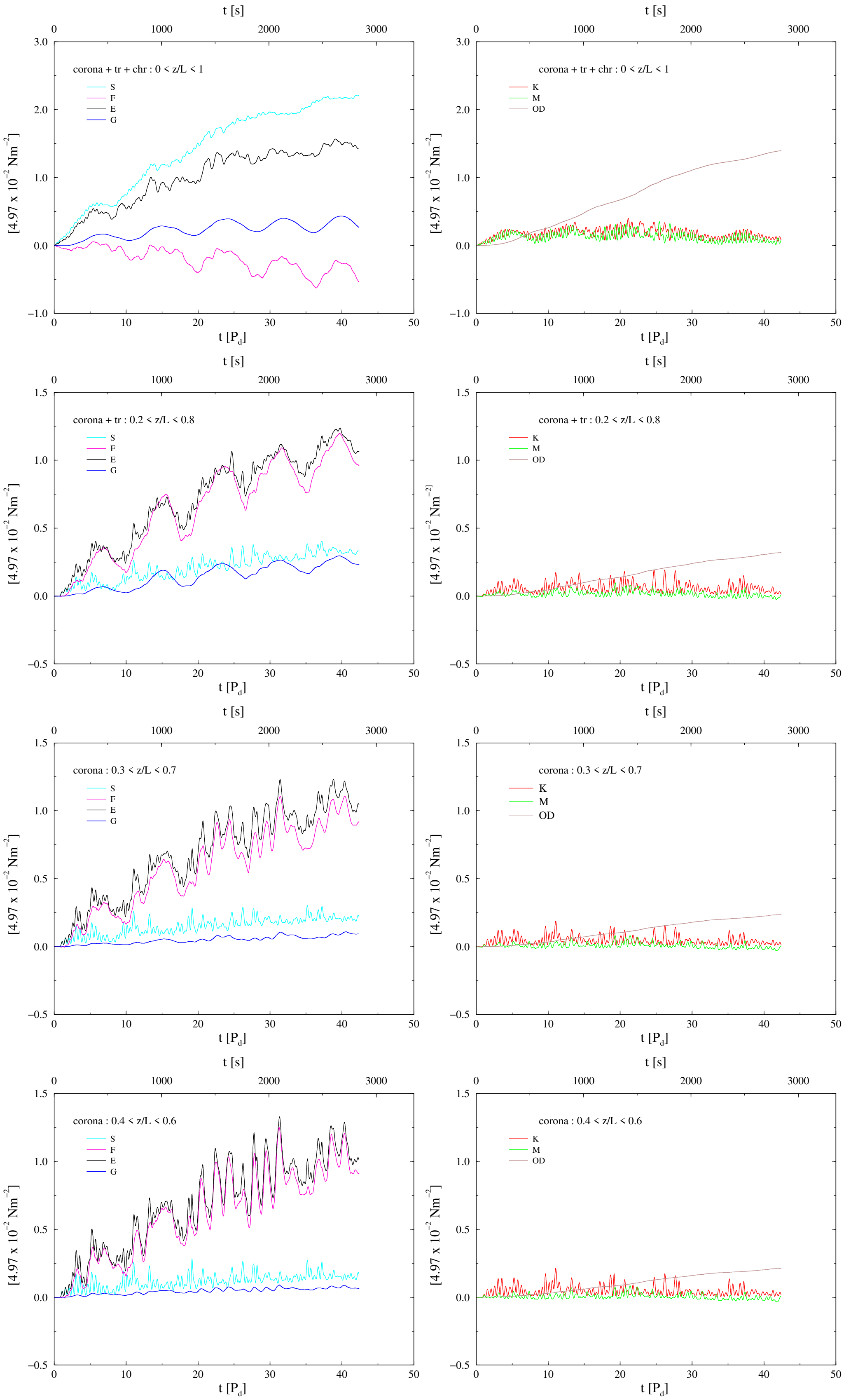

Figure 3. The evolution of the volume averaged energy balance quantities S, F, E, and G, for four different volumes (left panels). The evolution of the volume averaged kinetic energy K, magnetic energy M, and Ohmic dissipation OD for the same four volumes (right panels).

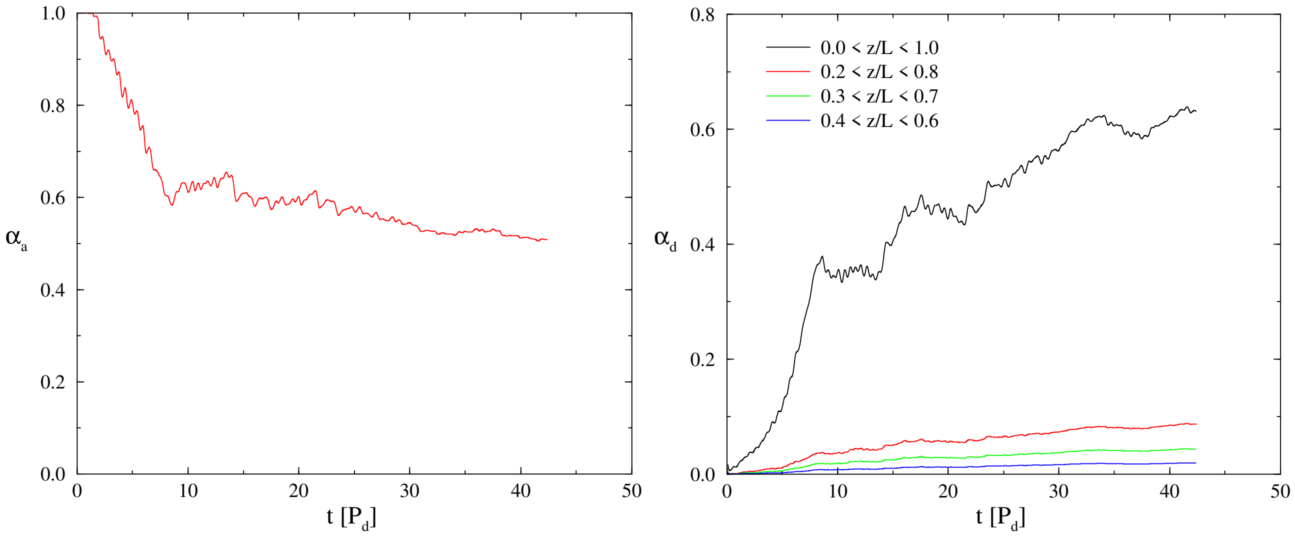

Figure 4. The heating efficiency as expressed by the absorption coefficient α_a (left) and the dissipation coefficient α_d (right). The dissipation coefficient is plotted for the same four volumes as used in Fig. 3.

field and velocity, but only after the heating efficiency has reached low values.

The fact that in our simulations the Alfvén waves predominantly generate slow magnetoacoustic waves that carry a significant amount of energy compared to the Alfvén waves and easily steepen into shocks strongly indicates that slow shock heating can be much more important for coronal heating than the direct heating through resonant absorption.

A more detailed account of our findings, including parameter scans of the Alfvén wave amplitude and period, and a simulation investigating the role of radiative losses and thermal conduction can be found in Beliën et al. (1999).

REFERENCES

Beliën, A.J.C., Martens, P.C.H., & Keppens, R. 1999, Astrophys. J., accepted

Berghmans, D., & De Bruyne, P. 1995, Astrophys. J., 453, 495

Browning, P.K. 1991, Plasma Phys. Contr. Nucl. Fusion, 33, 539

Davila, J.M. 1987, Astrophys. J., 317, 514

Goedbloed, J.P. 1995, in International Conf. on Plasma Physics, Foz do Iguacu, Brasil, Oct. 31 - Nov. 4, 1994, AIP Conference Proceedings (Am. Inst. Physics) 345, 465

Grossmann, W., & Smith, R.A. 1988, Astrophys. J., 332, 476

Halberstadt, G., & Goedbloed, J.P. 1995a, Astron. Astrophys., 301, 559

Halberstadt, G., & Goedbloed, J.P. 1995b, Astron. Astrophys., 301, 577

Hollweg, J.V. 1984, Solar Phys., 91, 269

Hollweg, J.V., & Yang, G. 1988, J. Geophys. Res., 93, 5423

Martens, P.C.H. 1986, in Coronal and Prominence Plasmas, NASA CP-2442, ed. A.I. Poland, 407

Ofman, L., Davila, J.M., & Steinolfson, R.S. 1994, Astrophys. J., 421, 360

Ofman, L., Davila, J.M., & Steinolfson, R.S. 1995, Astrophys. J., 444, 471.

Ofman, L., & Davila, J.M. 1995, J. Geophys. Res., 100, 23427

Ofman, L., Nakariakov, V. M., Deluca, E., Roberts, B., & Davila, J. M. 1999, American Astronomical Society Meeting, 194, 7909

Parker, E.N. 1992, J. Geophys. Res., 97, 4311

Poedts, S., & Kerner, W. 1992, J. Plasma Phys., 47, 139

Poedts, S., Beliën, A.J.C., & Goedbloed, J.P. 1994, Solar Phys., 151, 271

Poedts, S., & Boynton, G.C. 1996, Astron. Astrophys., 306, 610

Poedts, S., & Goedbloed, J.P. 1997, Astron. Astrophys., 321, 935

Roe, P.L. 1981, J. Comp. Phys., 43, 357

Ruderman, M.S., & Goossens, M. 1993, Solar Phys., 143, 69

Steinolfson, R.S., & Davila, J.M. 1993, Astrophys. J., 415, 354

Tóth, G. 1996, Astrophysical Letters & Communications, 34, 245

Zirker, J.B. 1993, Solar Phys., 148, 43